

## Nitrile-Rich Coordination Polymer $^1_{\infty}\{[\text{Fe}(\text{CH}_3\text{CN})_4(\text{pyrazine})](\text{ClO}_4)_2\}$ Exhibiting a HS $\rightleftharpoons$ LS Transition

Agata Białońska,<sup>†</sup> Robert Bronisz,<sup>\*,†</sup> Kamilla Darowska,<sup>†</sup> Krzysztof Drabent,<sup>†</sup> Joachim Kusz,<sup>‡</sup> Miłosz Siczek,<sup>†</sup> Marek Weselski,<sup>†</sup> Maciej Zubko,<sup>‡</sup> and Andrew Ozarowski<sup>§</sup>

<sup>†</sup>Faculty of Chemistry, University of Wrocław, F. Joliot-Curie 14, 50-383, Wrocław, Poland,

<sup>‡</sup>Institute of Physics, University of Silesia, PL-40007 Katowice, Poland, and <sup>§</sup>National High Magnetic Field Laboratory, Florida State University, Tallahassee, Florida 32310, United States

Received October 8, 2010

In a 1D network of  $^1_{\infty}\{[\text{Fe}(\text{CH}_3\text{CN})_4(\text{pyrazine})](\text{ClO}_4)_2\}$ , the presence of four neutral nitrile molecules besides the pyrazine donors in the first coordination sphere of iron(II) allows one to achieve a ligand field strength appropriate for the “spin-crossover” occurrence.

The construction of systems containing metal ions tethered by bridging ligand molecules into an infinite network is a fast-growing area because of interesting architectures and potential applications of such materials.<sup>1</sup> When a desired feature of a coordination network originates from the metal ion nature, a variation of the structural and donor properties of the ligands becomes the main tool for tuning of the material properties.<sup>2</sup> The spin-crossover (SCO) phenomenon<sup>3</sup> occurring in complexes of metal ions with  $3d^4$ – $3d^7$  electronic configuration is inherently related to the ligand field strength produced by the coordinated ligand molecules.<sup>4</sup> Iron(II) complexes are of great interest because in these systems abrupt  $\text{HS}(^5\text{T}_2) \rightleftharpoons \text{LS}(^1\text{A}_1)$

transitions (HS = high-spin and LS = low-spin), often accompanied by a hysteresis loop, are observed. SCO may be induced by a temperature change, pressure application, or light irradiation, and such materials are considered for potential applications as molecular switches, data storage, and displays<sup>5</sup> and in medicinal diagnostics.<sup>6</sup> Over the past decade, great attention was devoted to the preparation of polymeric SCO iron(II) systems based on cyanometalate anions because of their intriguing properties.<sup>7</sup> Several SCO systems containing polynitrile anions as bridging units were also prepared.<sup>8</sup> On the other hand, SCO complexes containing neutral organic nitriles in the first coordination sphere of iron(II) are rather scarce.<sup>9,10</sup> Recently, we have shown that, besides the complexes in which six 2-substituted tetrazole rings surround iron(II) ions, the 2-substituted tetrazoles are also prone to form SCO complexes comprising coordinated acetonitrile molecules.<sup>11</sup> A common feature of the known 2-substituted tetrazole-based SCO systems  $[\text{Fe}(\text{btz})_2(\text{CH}_3\text{CN})_2](\text{ClO}_4)_2 \cdot n\text{CH}_3\text{CN}$  [btz = 2-hydroxy-1-(tetrazol-1-yl)-3-(tetrazol-2-yl)propane and  $n = 2$  or btz = 1,6-di(tetrazol-2-yl)-hexane and  $n = 0$ ] and of iron(II) complexes with ligands including pyridine-like donor groups is that they contain no more than two coordinated nitrile molecules per metal ion. It is worth mentioning that, in complexes with bridging polynitrile anions such as dicyanamide and tricyanomethanide, no more than two nitrile groups, in addition to the pyridine-like donors, are required to reach a ligand field strength sufficient for the SCO occurrence.<sup>9</sup>

\*To whom correspondence should be addressed. E-mail: bron@wchuwr.pl.

(1) Kitagawa, S.; Kitaura, R.; Noro, S.-I. *Angew. Chem., Int. Ed.* **2004**, *43*, 2334.

(2) Elsevier, C. J.; Reedijk, J.; Walton, P. H.; Ward, M. D. *Dalton Trans.* **2003**, 1869.

(3) Gütllich, P.; Goodwin, H. A. *Top. Curr. Chem.* **2004**, 233, 1.

(4) Hauser, A. *Top. Curr. Chem.* **2004**, 233, 49.

(5) Letard, J. F.; Guionneau, P.; Goux-Capes, L. *Top. Curr. Chem.* **2004**, 235, 221.

(6) Muller, R. N.; Elst, L. V.; Laurent, S. J. *J. Am. Chem. Soc.* **2003**, *125*, 8405.

(7) (a) Bonhommeau, S.; Molnar, G.; Galet, A.; Zwick, A.; Real, J.-A.; McGarvey, J. J.; Bousseksou, A. *Angew. Chem., Int. Ed.* **2005**, *44*, 4069. (b) Bonhommeau, S.; Guillon, T.; Daku, L. M. L.; Demont, P.; Costa, J. S.; Letard, J. F.; Molnar, G.; Bousseksou, A. *Angew. Chem., Int. Ed.* **2006**, *45*, 1625. (c) Cobo, S.; Molnar, G.; Real, J.-A.; Bousseksou, A. *Angew. Chem., Int. Ed.* **2006**, *45*, 5786. (d) Boldog, I.; Gaspar, A. B.; Martinez, V.; Pardo-Ibanez, P.; Ksenofontov, V.; Bhattacharjee, A.; Gütllich, P.; Real, J.-A. *Angew. Chem., Int. Ed.* **2008**, *47*, 6433. (e) Larionova, J.; Salmon, L.; Guari, Y.; Tokarev, A.; Molvinger, K.; Molnar, G.; Bousseksou, A. *Angew. Chem., Int. Ed.* **2008**, *47*, 8236. (f) Ohba, M.; Yoneda, K.; Agusti, G.; Munoz, M. C.; Gaspar, A. B.; Real, J.-A.; Yamasaki, M.; Ando, H.; Nakao, Y.; Sakaki, S.; Kitagawa, S. *Angew. Chem., Int. Ed.* **2009**, *48*, 4767. (g) Agusti, G.; Ohtani, R.; Yoneda, K.; Gaspar, A. B.; Ohba, M.; Sanchez-Royo, J. F.; Munoz, M. C.; Kitagawa, S.; Real, J. A. *Angew. Chem., Int. Ed.* **2009**, *48*, 8944.

(8) (a) Genre, C.; Jeanneau, E.; Bousseksou, A.; Luneau, D.; Borshch, S. A.; Matouzenko, G. S. *Chem.—Eur. J.* **2008**, *14*, 697. (b) Ortega-Villar, N.; Thompson, A. L.; Munoz, M. C.; Ugalde-Saldivar, V. M.; Goeta, A. E.; Moreno-Esparza, R.; Real, J.-A. *Chem.—Eur. J.* **2005**, *11*, 5721. (c) Sheu, C.-F.; Pillet, S.; Lin, Y.-C.; Chen, S.-M.; Hsu, I.-J.; Lecomte, C.; Wang, Y. *Inorg. Chem.* **2008**, *47*, 10866.

(9) Batten, S. R.; Bjernemose, J.; Jensen, P.; Leita, B. A.; Murray, K. S.; Moubaraki, B.; Smith, J. P.; Toftlund, H. *Dalton Trans.* **2004**, 3370.

(10) (a) Quesada, M.; de Hoog, P.; Gamez, P.; Roubeau, O.; Aromí, G.; Donnadiou, B.; Massera, C.; Lutz, M.; Spek, A. L.; Reedijk, J. *Eur. J. Inorg. Chem.* **2006**, 1353. (b) Quesada, M.; de la Peña-O’Shea, V. A.; Aromí, G.; Geremia, S.; Massera, C.; Roubeau, O.; Gamez, P.; Reedijk, J. *Adv. Mater.* **2007**, *19*, 1397.

(11) (a) Białońska, A.; Bronisz, R.; Weselski, M. *Inorg. Chem.* **2008**, *47*, 4436. (b) Białońska, A.; Bronisz, R. *Inorg. Chem.* **2010**, *49*, 4534.

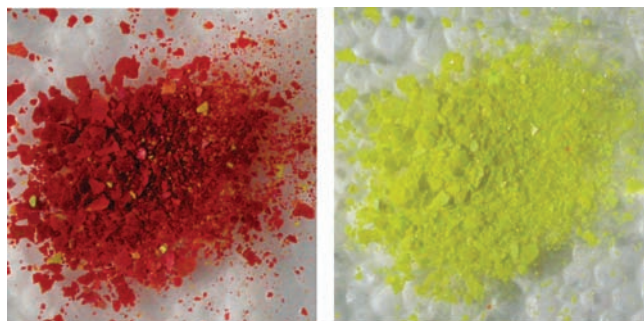


**Figure 1.** Change of color upon spin transition in **1** (reddish-violet, LS form; yellow, HS form).

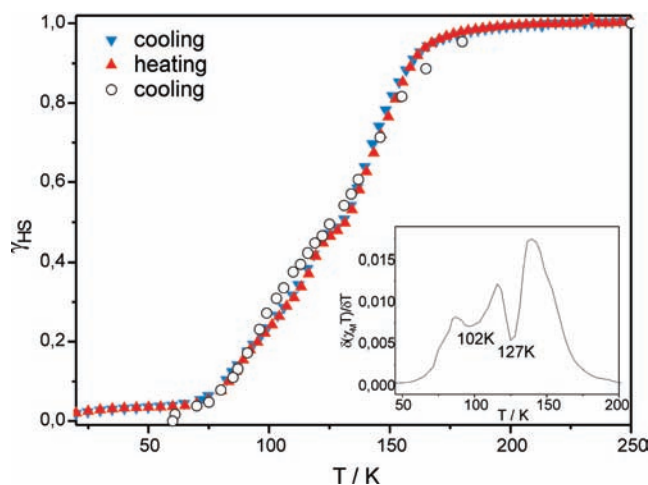


**Figure 2.**  $\gamma_{\text{HS}}$  vs  $T$  dependence for **1** deduced from the magnetic susceptibility measurements performed in cooling (down triangles) and warming (up triangles) modes and from the Mossbauer spectra measured in cooling mode (circles). The inset shows the  $\delta(\chi_{\text{M}}T)/\delta T$  curve.

In this Communication, we report a novel nitrile-rich SCO system,  $[\text{Fe}(\text{CH}_3\text{CN})_4(\text{pyz})](\text{ClO}_4)_2$  (**1**; pyz = pyrazine). **1** was prepared in the reaction of pyrazine with  $\text{Fe}(\text{ClO}_4)_2 \cdot 6\text{H}_2\text{O}$  carried out in acetonitrile.<sup>12</sup> The product crystallizes as yellow triclinic crystals, which are stable under a nitrogen atmosphere but, when exposed to atmospheric humidity, become cloudy within 1 h. Crystals of **1** change color from yellow to reddish-violet upon immersion in liquid nitrogen (Figure 1), suggesting a thermally induced HS  $\rightarrow$  LS transition. The thermochromic effect in such systems results from the spin-allowed  $^1\text{A}_1 \rightarrow ^1\text{T}_1$  d–d transition in the LS form.

In order to confirm the spin transition in **1**, the magnetic susceptibility was measured over the temperature range 5–300 K (Figure 2). The sample was placed in a sealed glass tube to protect it from humidity. The  $\chi_{\text{M}}T$  value, which is almost constant over the temperature range 300–170 K at  $3.4 \text{ cm}^3 \text{ Kmol}^{-1}$ , is consistent with that of the HS state of iron(II).

Upon further lowering of the temperature, a three-stage spin transition is observed, with the first steep segment centered at

the critical temperature  $T_{1/2}^{(1)}$  of 146 K. The next stage, between 135 and 120 K, is less steep with an inflection point at 127 K. At that temperature,  $\chi_{\text{M}}T$  of  $1.71 \text{ cm}^3 \text{ Kmol}^{-1}$  is observed, indicating a 50% HS  $\rightarrow$  LS conversion ( $\gamma_{\text{HS}} = 0.50$ ). The decrease of  $\chi_{\text{M}}T$  below 120 K is more abrupt again.

Inspection of the first derivative  $\delta(\chi_{\text{M}}T)/\delta T$  (see the inset in Figure 2) indicates a second inflection point at 102 K. At this temperature, the value of  $\chi_{\text{M}}T$  equals  $0.88 \text{ cm}^3 \text{ Kmol}^{-1}$  and  $\gamma_{\text{HS}} = 0.26$  is deduced from the equation  $\chi_{\text{M}}T - (\chi_{\text{M}}T)_{\text{LS}} / [(\chi_{\text{M}}T)_{\text{HS}} - (\chi_{\text{M}}T)_{\text{LS}}]$  [where  $(\chi_{\text{M}}T)_{\text{LS}} = 3.4 \text{ cm}^3 \text{ Kmol}^{-1}$  and  $(\chi_{\text{M}}T)_{\text{HS}} = 0$ ]. Further lowering of the temperature causes a more gradual spin transition, which is accomplished at 75 K. Taking into account localization of the second inflection point, the critical temperatures  $T_{1/2}^{(2)}$  and  $T_{1/2}^{(3)}$  for the second and third steps of the spin transition may be estimated as equal to 115 K ( $\gamma_{\text{HS}} \approx 0.38$ ) and 85 K ( $\gamma_{\text{HS}} \approx 0.12$ ), respectively. In the heating mode, the  $\chi_{\text{M}}T$  vs  $T$  dependence for the third step is the same as that in the cooling mode, while the second and first steps are shifted toward higher temperatures by approximately 2 and 3 K, respectively, thus exhibiting narrow hysteresis loops.

The Mössbauer spectra of complex **1** were recorded over the temperature range from 300 to 60 K (Figure S1 in the Supporting Information). At 296 K, the Mössbauer spectrum shows a symmetrical doublet (HS<sub>1</sub>) with an isomer shift  $\delta = 0.972(5) \text{ mm s}^{-1}$  and a quadrupole splitting  $\Delta E_{\text{Q}} = 0.954(4) \text{ mm s}^{-1}$ , typical for HS iron(II). At 180 K, a second doublet (HS<sub>2</sub>) appears, with  $\delta = 1.083(3) \text{ mm s}^{-1}$  and  $\Delta E_{\text{Q}} = 3.228(4) \text{ mm s}^{-1}$ . A reaction product of **1** with atmospheric water vapor (see Figure S2 and Table S2 in the Supporting Information) exhibits identical parameters. This impurity is SCO-inactive, and its relative contribution (about 8% of the relative area) remains practically unchanged at lower temperatures. At 165 K, a third, slightly split doublet appears, with  $\delta = 0.43(3) \text{ mm s}^{-1}$  and  $\Delta E_{\text{Q}} = 0.11(6) \text{ mm s}^{-1}$ , characteristic for LS iron(II). Further lowering of the temperature causes a gradual decrease of the main doublet HS<sub>1</sub> area and a corresponding growth of the LS component area (Table S1 in the Supporting Information). The presence of a second LS phase [a singlet with  $\delta = 0.58(4) \text{ mm s}^{-1}$ ] was detected below 155 K. That species disappears below 75 K. The HS<sub>1</sub> doublet is practically absent below 60 K, indicating a complete HS  $\rightarrow$  LS transition in **1**. In summary, the temperature dependence of the HS and LS fractions obtained from Mössbauer studies is in agreement with the magnetic susceptibility temperature dependence.

X-ray measurements for **1** were performed at temperatures of 180(1), 127(1), 115(1), 102(1), and 80(1) K (see the Supporting Information). The complex crystallizes in the orthorhombic system, space group  $Pccn$ , and is isostructural with  $[\text{Cu}(\text{CH}_3\text{CN})_4(\text{pyz})](\text{ClO}_4)_2$ .<sup>13</sup> There is one crystallographically independent iron(II) site. Two neighboring iron(II) ions, located on the 2-fold axis, are bridged by one pyrazine molecule coordinating via the nitrogen atoms N and N'. This bridging mode is propagated along the  $c$  direction, which leads to the formation of a 1D polymeric chain (Figure 3). Rectangular motif of the arrangement of 1D chains is observed perpendicularly to the  $c$  axis. At 180 K, the Fe–N(pyrazine) bond lengths are equal to 2.162 and 2.167 Å. The coordination sphere of the iron(II) ions is completed by four acetonitrile molecules with two sets of Fe–N(CH<sub>3</sub>CN) bond

(12) Synthesis of **1** was performed under a nitrogen atmosphere using a standard Schlenk technique.  $\text{Fe}(\text{ClO}_4)_2 \cdot 6\text{H}_2\text{O}$  (0.6 mmol, 216.0 mg) dissolved in  $\text{CH}_3\text{CN}$  (2.5 mL) was added to the solution of pyrazine (1.2 mmol, 96.0 mg) in  $\text{CH}_3\text{CN}$  (2.5 mL), and the resulting pale-yellow reaction mixture was left in the closed Schlenk flask. After 24 h, yellow crystals of **1** were filtered off and dried in a nitrogen atmosphere. Yield: 87.1 mg (29%). Anal. Calcd for  $\text{FeC}_{12}\text{H}_{16}\text{N}_6\text{Cl}_2\text{O}_8$ : C, 28.9; H, 3.2; N, 16.8. Found: C, 28.4; H, 3.3; N, 16.6.

(13) Begley, M. J.; Hubberstey, P.; Stroud, J. J. *J. Chem. Soc., Dalton Trans.* **1996**, 2323.

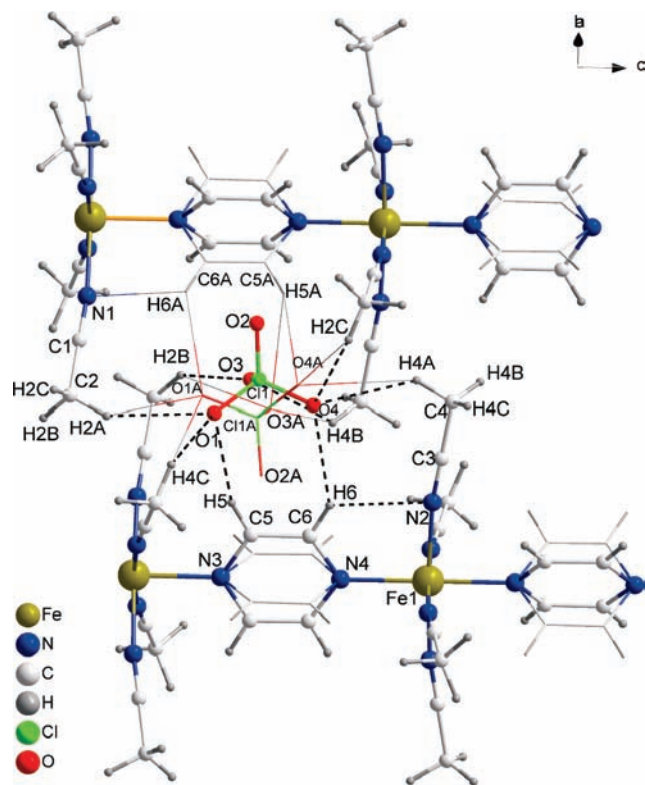


**Figure 3.** Perspective view of the 1D polymeric chains in **1** at 115 K showing the scheme of intermolecular interactions between molecules dominating over the whole temperature range (dashed lines) and molecules occupying alternative positions (thin solid lines).

lengths of 2.151 and 2.169 Å. Therefore, the  $\text{FeN}_6$  chromophore exhibits the geometry of a slightly distorted octahedron with  $\text{Fe-N}$  distances typical for the HS form. Lowering of the temperature causes shortening of the metal–ligand bond lengths, indicating the HS  $\rightarrow$  LS transition. Thus, at 80 K, the  $\text{Fe-N}(\text{pyrazine})$  and  $\text{Fe-N}(\text{CH}_3\text{CN})$  bond lengths are equal to 1.998, 2.023 and 1.943, 1.951 Å, respectively. The average values of the  $\text{Fe-N}$  distances at intermediate temperatures 127 K (2.075, 2.079 and 2.042, 2.048 Å) and 102 K (2.027, 2.050 and 1.983, 1.994 Å), corresponding to the inflection points, are shortened with relation to the  $\text{Fe-N}$  bond lengths at 80 K (calculated as  $[d(\text{Fe-N})_{\text{T}} - d(\text{Fe-N})_{\text{LS}}]/[d(\text{Fe-N})_{\text{HS}} - d(\text{Fe-N})_{\text{LS}}]$ ) by about 55 and 82%. The HS  $\rightarrow$  LS transition is associated with a shortening of the distances between the bridged iron(II) ions, which are 7.109, 6.962, 6.883, and 6.828 Å at temperatures 180, 127, 102, and 80 K, respectively. Also, the shortest distance between iron(II) ions from neighboring chains  $\text{Fe}\cdots\text{Fe}(1-x, 1-y, -z)$  decreases from 8.501 (180 K), to 8.455 (127 K), to 8.430 (102 K), to 8.409 Å (80 K). There are no direct intermolecular interactions between the chains. Interactions are mediated by anions arranged in layers parallel to the  $bc$  plane. The perchlorate anions are engaged in intermolecular interactions with the pyrazine and acetonitrile moieties coming

from neighboring 1D chains, which are arranged along the  $[1, 1, 0]$  direction. In this way, 2D supramolecular layers are formed. The perchlorates interact also with the coordinated acetonitrile molecules from adjoining 2D layers, extending the structure into a 3D supramolecular architecture. The number of intermolecular contacts at 127 K remains the same as that observed at 180 K, but the respective distances are altered slightly (Table S3 in the Supporting Information). Lowering of the temperature from 127 to 115 K causes disordering of the pyrazine ring, and even a more severe disordering of the perchlorate anions. At 115 K, about 12% of the anions and pyrazine moieties occupy the alternative positions. At 102 K, the fraction of disordered molecules increases to about 18%. The structural processes described above are accompanied by a reorganization of the existing intermolecular contacts and the appearance of novel ones. An additional contact,  $\text{C2-H2B}\cdots\text{O2A}$  ( $2-x, 1/2+y, 1/2-z$ ), is formed between the 2D supramolecular layers (Table S4 in the Supporting Information). Moreover, below 127 K, a second orientation of the pyrazine ring is additionally stabilized by a new intermolecular interaction,  $\text{C6A-H6A}\cdots\text{O1A}$  ( $1/2+x, 1-y, 1/2-z$ ). It is worth mentioning that both positions of the pyrazine rings are favored by the  $\text{C}_{\text{pyrazine}}-\text{H}\cdots\text{N}_{\text{acetonitrile}}$  intramolecular interaction. A further temperature decrease down to 80 K does not involve any structural changes in the polymeric backbone, and the number of contacts remains unchanged. Surprisingly, below 102 K, the disorder increases only very slowly, so that at 80 K, only about 20% of the molecules occupy the respective alternative positions.

In conclusion, we report on the first example of a SCO material in which the presence of four neutral nitrile molecules besides pyrazine in the coordination sphere of iron(II) allowed one to reach a ligand field strength sufficient for the spin transition. SCO in **1** occurs in three poorly resolved steps and is accompanied by intermolecular contact reorganization and by the order–disorder phenomenon. It was revealed that the structural evolution proceeds in consecutive stages, consisting first of the disorder appearance starting at ca. 127 K, next of a continuous increase of the disordered fraction upon cooling from 127 to 102 K, and finally inhibition of a further disorder increase below 102 K.

**Acknowledgment.** We thank the Ministry of Science and Higher Education of Poland for their financial support of this research (Grant 2493/B/H03/2008/34). The Mössbauer spectra were recorded at the NHMFL, which is funded by the NSF through Cooperative Agreement No. DMR-0654118, the State of Florida, and the DOE.

**Supporting Information Available:** Crystallographic details, X-ray crystallographic files in CIF format, figures of Mössbauer spectra for **1** and product reaction of **1** with water, and tables containing Mössbauer parameters and inter- and intramolecular contacts for **1**. This material is available free of charge via the Internet at <http://pubs.acs.org>.